A preliminary study of global and diffuse solar radiation data from a SONDA station located in São Martinho da Serra, RS - Brazil (29.44ºS, 53.82ºW)

Ricardo André Guarnieri*,[1], Leonardo Biazi[2], Nelson Jorge Schuch[2], Sylvio Luiz Mantelli Neto[1], Enio Bueno Pereira[1]
[1]Instituto Nacional de Pesquisas Espaciais – Centro de Previsão de Tempo e Estudos Climáticos – DMA/CPTEC/INPE
[2]Instituto Nacional de Pesquisas Espaciais – Unidade Regional Sul de Pesquisas Espaciais – RSU/INPE

This paper was prepared for presentation at the 9th International Congress of the Brazilian Geophysical Society held in Salvador, Brazil, 11-14 September 2005.

Abstract

The aim of this work is to present a preliminary study of the incident solar radiation data, measured by the SONDA station of São Martinho da Serra, RS, Brazil. The global solar radiation and one of its components, the diffuse radiation, are compared each other and with some correlations and results found in the technical literature. Data produced by pyranometers in the period from July/2004 (station installation) to March/2005 were used. It was found a good agreement between the observational data and results already published. Some of the observed differences were discussed. However, a longer period of data is necessary in order to create models correlating the global and diffuse radiation for this station.

Introduction

The radiant energy emitted by the sun is practically the only source of energy that influences atmospheric motions and several processes in the atmosphere and surface layers of the Earth's crust (Kondratyev, 1969). The Sun emits radiation in all wavelengths of the electromagnetic spectrum, approximately following the Planck law. The solar spectrum is a continuum with a maximum situated in the visible region, with a curve similar to a blackbody emitting at 6000 K (Coulson, 1975; Liou, 1980; Brasseur and Solomon, 1986; Lenoble,1993).

Accordingly to Liou (1980), the amount of total solar energy (whole solar spectrum) reaching the top of atmosphere is called *solar constant* (S). It is defined as the flux of solar energy (energy per time) across a surface of unit area (or *irradiance*) normal to the solar beam at the mean distance between the sun and earth. It is approximately equal to the annual average of total irradiance reaching the top of atmosphere, and its value is about 1368 W m^{-2}. Due to the eccentricity of the earth's orbit around the Sun, the solar irradiance varies ± 3.4% from *S* during the year. The solar constant also follows the 11-year sunspot cycle, varying about ± 0.6 W m^{-2} (Kidder and Vonder Haar, 1995).

The energy carried by solar radiation lies almost totally at the visible and near-infrared regions of the electromagnetic spectrum. About 99% of the energy occurs at wavelengths (λ) shorter than 4 μm, with a maximum of intensity in approximately 0.5 μm (Hoyt and Schatten, 1997). According to Lutgens and Tarbuck (1995), approximately 43% of the total energy carried by solar radiation lies in the visible region (0.4 – 0.7 μm), about 49% in the near-infrared region (λ > 0.7 μm) and about 7% in the ultraviolet region (λ < 0.4 μm). Less than 1% of the solar radiation is emitted in X-rays, gamma rays or radio waves.

After reach the top of atmosphere and penetrate it, the solar radiation interacts with the atmospheric constituents, clouds and the planet surface. The main processes that affect the intensity of the incident solar radiation are absorption and scattering (Liou, 1980). The atmospheric absorption in the visible wavelengths is quite weak. So, we can consider the atmosphere practically transparent to solar radiation.

Scattering is a physical process in which a particle in the path of an electromagnetic wave continuously removes energy from the incident wave. This energy is dispersed in all directions, acting as a punctual source of scattered energy. This scattered energy is still radiation, being only removed from the incidence direction. But, since part of the solar energy is scattered backward, the amount of energy that reaches the surface is attenuated (Peixoto and Oort, 1992). In the atmosphere, the particles that causes scattering have sizes in the range from the gas molecules of air (~ 10^8 cm) to the large raindrops and hailstones (~ 1 cm) (Liou, 1980).

The ratio between the scattering particle size and the incident radiation wavelength determines the scattering regimes. When particles are much smaller than the wavelength, the scattering is called *Rayleigh scattering*. For particles with sizes comparable to or larger than the wavelength, the scattering is referred as *Mie scattering*. If the particle size is much greater than wavelength, then the deviation of the incident radiation is explained by geometric optics (Liou, 1980).

The scattering caused by atmospheric air molecules lies in the Rayleigh regime, following an inverse power law of the wavelength (Scattering ~ $1/\lambda^4$). The Mie regime usually comprises the scattering of solar radiation by particles of haze, smoke, smog, dust and other aerosols. There are no dependency between scattering intensity and wavelengths. Finally the scattering of visible radiation by cloud droplets, raindrops and ice particles can be described by the principles of geometric optics (Wallace and Hobbs, 1977; Liou, 1980; Kidder and Vonder Haar, 1995).

After cross a layer with scattering agents, like the atmosphere, the solar irradiance that reaches the surface

can be divided in two components. The first part is the component coming directly from the source direction – *direct irradiance*. The second component comprises the radiation coming from all other directions of the sky due to scattering – *diffuse irradiance*. The sum of these two components is called *global irradiance*. The diffuse component consists of scattering by air molecules, aerosols and clouds. Clouds can attenuate or increase the global radiation depending on the type, optical properties, amount, thickness, position and number of layers (Iqbal, 1983).

The study of the available incident solar irradiance, its components, and its variability is important for the solar energy assessment for renewable energy applications. To attend the demand of solar and wind data necessary to energy projects in Brazil, it was created a project called SONDA – *Sistema de Organização Nacional de Dados Ambientais* or System of National Organization of Environmental Data – with the aim of install several stations equipped with radiometers and wind-meters, and collect data. The solar radiation data produced will be important not only to energy assessment but also to meteorological researches, especially about climate and climate changes, as well as other applications.

In this work only some preliminary results are presented. The data were compared with some published models that calculate the diffuse radiation from global radiation.

Methodology

The radiation data were collected by a SONDA station located in the southern part of Brazil, in a city called São Martinho da Serra – RS, more specifically at the *Observatório Espacial do Sul – OES/RSU/INPE-MCT* – 29.44ºS, 53.82ºW. SONDA is a project coordinated by the *Instituto Nacional de Pesquisas Espaciais – INPE-MCT*, through its *Centro de Previsão de Tempo e Estudos Climáticos – CPTEC/INPE-MCT*.

The São Martinho da Serra SONDA station was installed on July/2004. Besides the several instruments, the station has two pyranometers: Kipp & Zonen CM21 Pyranometer and Kipp & Zonen CM22 Pyranometer. The CM21 model is used to measure the global radiation between 0.3 and 2.8 µm, narrow band. The CM22 model can measure the global radiation, but it was projected and has been used for diffuse radiation measurements between 0.2 and 3.6 µm. For diffuse radiation measurements, the CM22 is mounted on a Kipp & Zonen Two Axis Positioner - 2AP that tracks the Sun continuously, occulting the solar disk using a small ball that shades the sensor from the direct solar radiation. The Figure1 shows the platform where the equipments are mounted and, in detail, the CM21 and CM22 pyranometers.

The instruments produce data with 1-second temporal resolution, but the data are averaged each 60 seconds and stored with 1-minute resolution. In this work the data were integrated along a period of a day. So, all global and diffuse radiation data used in this work are daily total energy, expressed in Joules per square meter, $J\ m^{-2}$. Along the text, these quantities will be referred as "daily global radiation" and "daily diffuse radiation", and represented, respectively, by H and H_d.

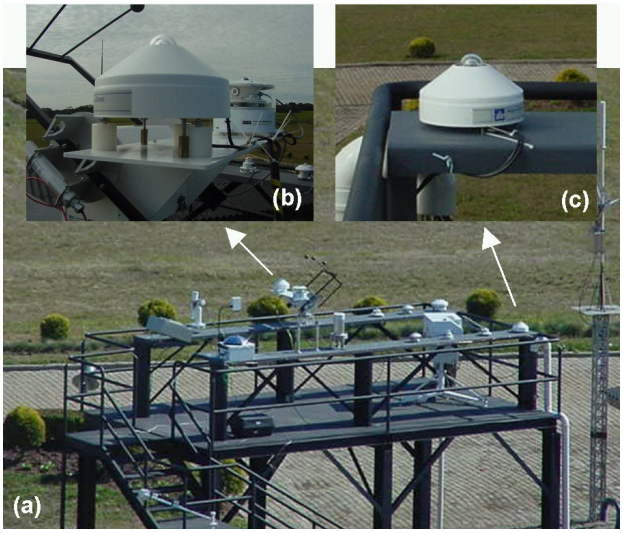

Figure 1 – (a) Platform where the instrumens of SONDA station and other instruments for UV radiation and ozone measurements are installed at Observatório Espacial do Sul, São Martinho da Serra; (b) CM22 Pyranometer installed on 2AP Positioner; (c) CM21 Pyranometer.

In order to obtain adimensional parameters, the "daily radiations" were normalized by the total daily energy incident in the top of atmosphere (TOA), referred only by "daily TOA radiation", represented by H_0 and calculated with the expression (Iqbal, 1983):

$$H_0 = \frac{1368}{\pi}\left(\frac{d_m}{d}\right)^2 [h_0 \operatorname{sen}(\varphi)\operatorname{sen}(\delta) + \cos(\varphi)\cos(\delta)\operatorname{sen}(h_0)] \quad (1)$$

where "1368" is the solar constant value in $W\ m^{-2}$, $(d_m/d)^2$ is the eccentricity factor, d_m is the mean distance between Sun and earth, d is the earth-Sun distance for the day in which we want to obtain H_0, φ is the station latitude, δ is the solar declination, and h_0 is the sunrise/sunset hour angle. The eccentricity factor and solar declination can be calculated for each day of year using the equations presented by Spencer (1971). The sunrise/sunset hour angle is a function of latitude and declination.

Using H and H_0 data, the *clearness parameter* for an individual day, K_T, is defined as (Iqbal, 1983):

$$K_T = \frac{H}{H_0} \quad (2)$$

Similar ratios between H_d and H_0 and between H_d and H were also performed, and they are represented by K_d and K, respectively. According to Iqbal (1983), on a cloudy day, the global radiation received is an indicative of the cloudiness extent and so the diffuse radiation amount. At a given location, the parameter K_T is an indicative of the daily clearness, and the K parameter also gives an indication of the diffuse radiation amount.

As an attempt to create a simple model to predict the value of H_d from a given value of H for an individual day, some researchers tried to establish correlations between H/H_0 (K_T) and H_d/H (K) (Liu and Jordan, 1960; Ruth and Chant, 1976; Collares-Pereira and Rabl, 1979). Iqbal (1983) presented some of these correlations.

Ruth and Chant used several years of pyranometers radiation data from four stations of the Canadian network. From the results published by Ruth and Chant, Iqbal (1979) determined the following analytical expression, referred from now on as *RC correlation*:

$$\frac{H_d}{H} = \begin{cases} 0.98 \\ (K_T \le 0.1) \\ 1.910 + 1.154K_T - 4.936K_T^2 + 2.848K_T^3 \\ (0.1 \le K_T \le 0.7) \end{cases} \quad (3)$$

Collares-Pereira and Rabl used pyrheliometer data of a very short period from five stations located in the United States and determined an analytical expression referred as *CPR correlation*:

$$\frac{H_d}{H} = \begin{cases} 0.99 \\ (K_T \le 0.17) \\ 1.188 - 2.272K_T + 9.473K_T^2 - 21.856K_T^3 + 14.648K_T^4 \\ (0.17 \le K_T \le 0.8) \end{cases} \quad (4)$$

Iqbal (1983) compared these two correlations and observed that the differences between them are small. Both studies were performed with data from stations located from 31º to 53º N latitude. According to Iqbal, the closeness of the two correlations demonstrates that within this range, latitude effects are minimal on the both studies. Plotting these correlations, Iqbal observed that under very cloudy conditions ($K_T \rightarrow 0$), global radiation is composed mainly by diffuse radiation. On very clear days, about 20% of the daily radiation is diffuse. For comparison, the values of K_T and K calculated in the present work were plotted with the RC and CPR correlations.

Another way of study daily diffuse radiation is through the correlation of H/H_0 (K_T) with H_d/H_0 (K_d). Figure 2 shows a plot presented by Iqbal (1983), in which is defined three possible sky conditions: very cloudy, partly cloudy, and clear skies. The data used in the present work were compared with the Iqbal's plot shown on this figure. Iqbal emphasizes that during very cloudy days, diffuse radiation is equal to global radiation. Also, during partly cloudy days, diffuse radiation is between 20 and 35% of its extraterrestrial value. During clear days, the diffuse radiation is about half the value expected for partly cloudy days.

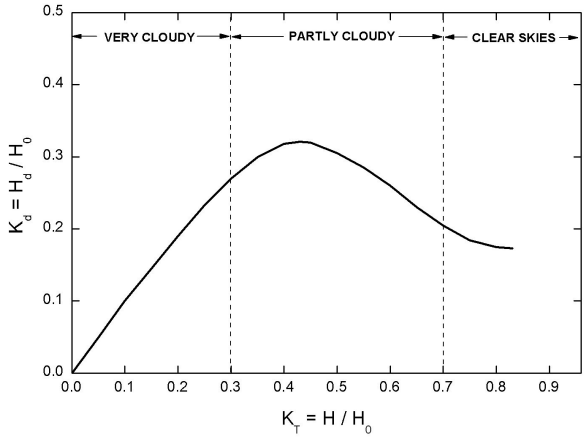

Figure 2 –Daily diffuse radiation variation as function of the clearness index. Adapted from Iqbal (1983).

The period of data used in this work was from July 17th, 2004 to March 31st, 2005. The data for some days in October/2004 were not used because there was a failure in the Sun occulting and consequent wrong diffuse radiation measurement. In this study, a total of 232 days with good quality data were used.

Results

For each day of data, curves for global and diffuse measured radiation were plotted. The integration over each period of one day (1440 minutes) was performed and the daily integrals were obtained. The Figure 3 shows the irradiance curves for some analyzed days. These specific days summarize the four more common situations observed: (a) clear sky (without noise in the global radiation curve); (b) clear sky with a few clouds (with noise in the global radiation curve); (c) cloudy sky; (d) hard cloudy sky (the diffuse radiation curve almost completely superposed to the global radiation curve). The values for daily integrals, the solar irradiance at the TOA, and the ratios among the daily integrals are shown in the figure.

It can be observed in Figure 3 that in days without clouds (a), the diffuse radiation is small compared with the global radiation. In Figure 3(b) the noises in the global radiation curve occur simultaneously with an increase in diffuse radiation. It possibly happens because clouds scatter the direct component, reducing the global and increasing the diffuse radiation. In a cloudy day, as shown on Figure 3(c), the global irradiances are reduced along the whole day, while the diffuse radiation is increased. Finally, during days with hard cloudy conditions, the diffuse radiation is almost equal to the global radiation, as shown in Figure 3(d). For this case, the direct component is totally scattered, and almost all radiation that reaches the surface is diffuse.

In Figure 4, the daily global radiation and daily diffuse radiation obtained from the pyranometer measurements were plotted with the calculated daily TOA radiation. The shaded area bellow the TOA radiation curve represents the amount of solar radiation backscattered to space by the atmosphere. As previously stated, there is a period of data not used on October/2004 due to a failure in the measurement of diffuse radiation.

The K_T, K_d and K parameters were calculated from the daily integrals. The parameter K was plotted as function of K_T on Figure 5. This figure also shows the curves generated using the RC and CPR correlations, according to equations (3) and (4). The data presented a similar behavior compared with both correlations. Days with clear sky ($K_T > 0.7$) presented values for K smaller than the ones calculated by CPR correlation. This results that a small fraction of diffuse radiation was observed in clear sky days, compared with that calculated by the theoretical model. Only a few points have a spurious behavior, and they were marked with arrows in the figure.

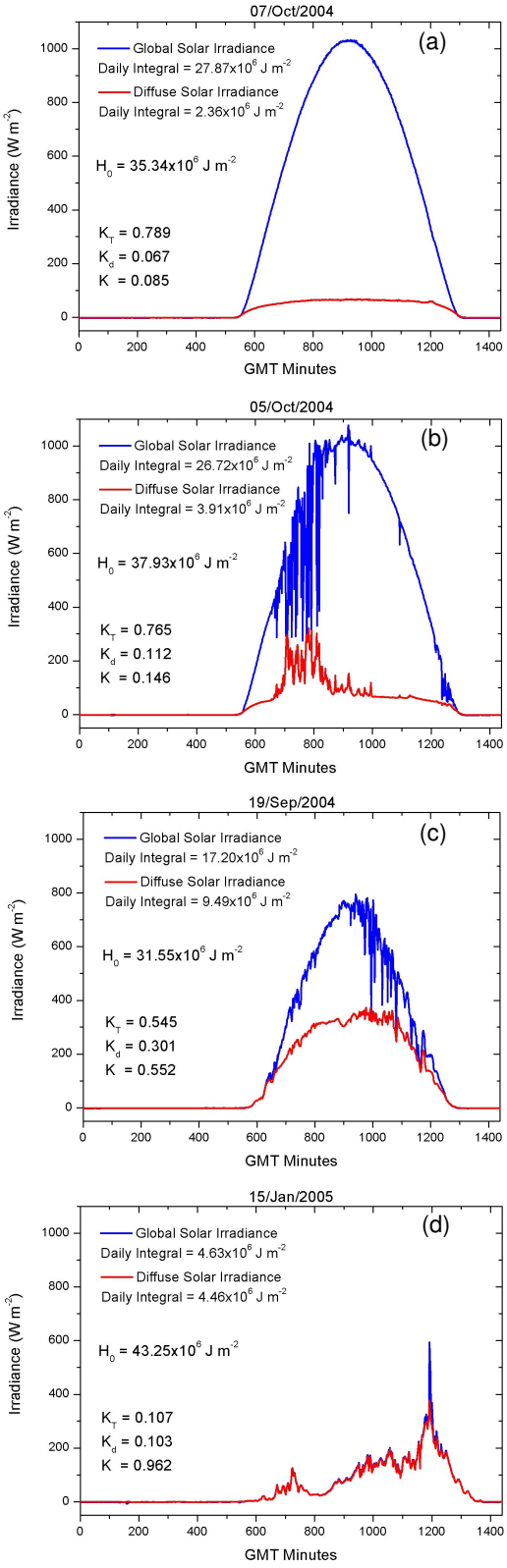

Figure 3 – Irradiance curves plotted from the pyranometers measurements for some days: (a) without clouds; (b) few clouds; (c) cloudy; (d) hard cloudy. The values for daily global and diffuse radiation, H_0, K_T (H/H_0), K_d(H_d/H_0), and K(H_d/H) are also shown.

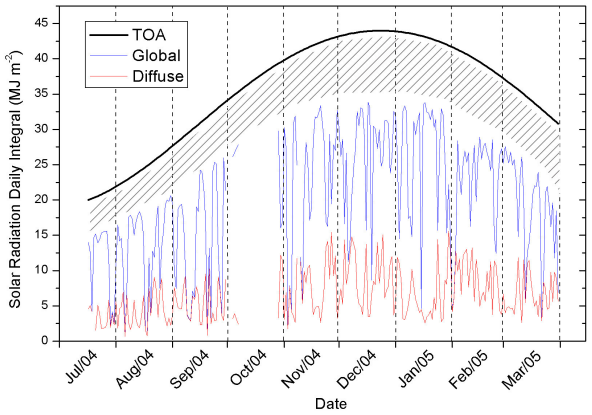

Figure 4 – Daily TOA, global and diffuse radiation for the whole data period used (1 MJ = $1x10^6$ J = 277.77 W h).

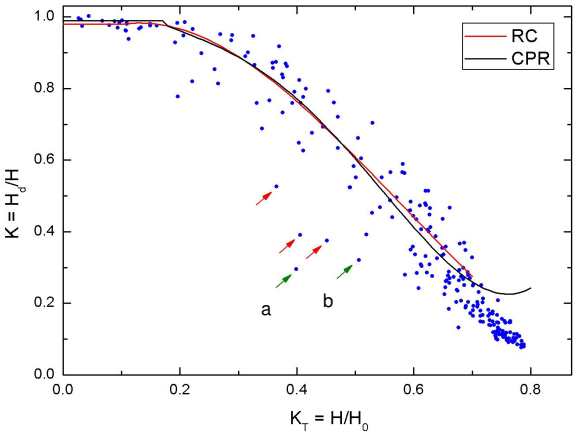

Figure 5 – Fraction of diffuse radiation (K) as function of clearness paramenter (K_T) and the correlations of Ruth and Chant (RC) and Collares-Pereira and Rabl (CPR).

Figure 6 has the K_d values plotted with K_T values as an attempt to observe a similar behavior as presented on Figure 2. Some points are separated from the group that follows the general behavior. These points are exactly the same ones marked with arrows on Figure 5, and were again marked here. Clear sky days presented diffuse radiation values smaller than that estimated by Iqbal.

The points showing a spurious behavior (marked with arrows on Figures 5 and 6), compared to the whole set of data and the theoretical curves, were days with opposite extremes of cloudiness along the day. In Figure 7, two examples of this kind of day are shown, corresponding to those days pointed with green arrows on Figure 5 and 6: day 08/Jan/2005 (green arrow *a*) and day 06/Feb/2005 (green arrow *b*). A curve for the nearest clear sky day (gray line) was plotted for each example, for comparison.

On Figures 5 and 6, for K_T > 0.7 (clear sky days), the difference observed between the data and the theoretical values can be explained by the latitude difference. While the RC and CPR correlations, as well as the Iqbal's curve (Figure 2), were made with data from several stations between 31º to 53º N latitude, the data used in this work were obtained from a station at 29.44º S latitude. For higher latitudes the slant path crossed by the solar

radiation through the atmosphere is longer, occurring more effective scattering and increasing the diffuse component. Other possible explanation to these deviations is the existence of atmospheric differences among the stations. Stations located in polluted places or exposed to other sources of aerosols may present an enhanced amount of diffuse radiation in clear sky days because the scattering caused by these particles (Mie scattering).

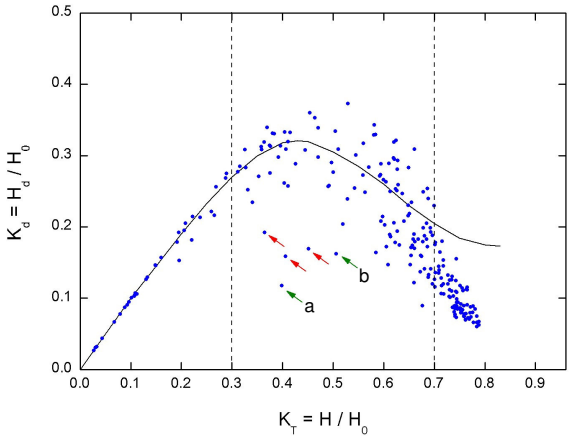

Figure 6 - Variation of the daily diffuse radiation as a function of the clearness index according to Iqbal (1983) – black line – and daily values for K_T and K_d determined from the pyranometers measurements – blue points.

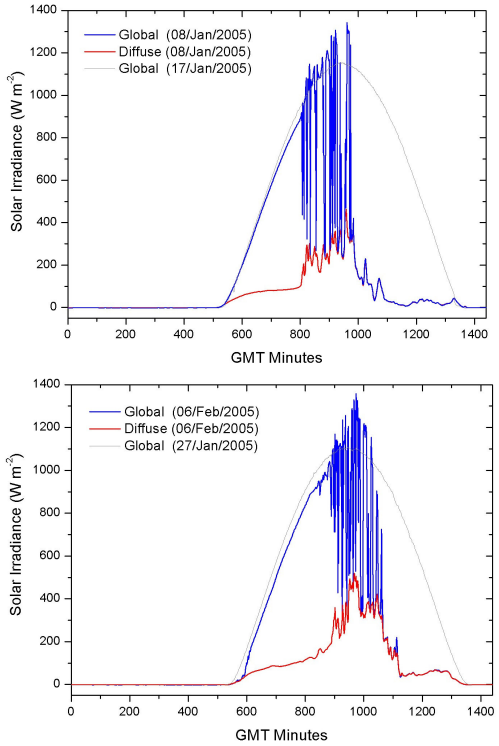

Figure 7 – Two examples of days with opposite extremes of cloudiness in the same day (blue and red lines for global and diffuse radiation, respectively). For each example, a curve for the nearest clear sky day (gray line) is plotted for comparison.

The histogram on Figure 8(a) shows the number of days in each clearness parameter interval. Using the same criteria from Iqbal (1983), the number of days with clear sky, partly cloudy and very cloudy were accounted and are summarized in the box. The Figure 8(b) are the same histogram but with percentage values.

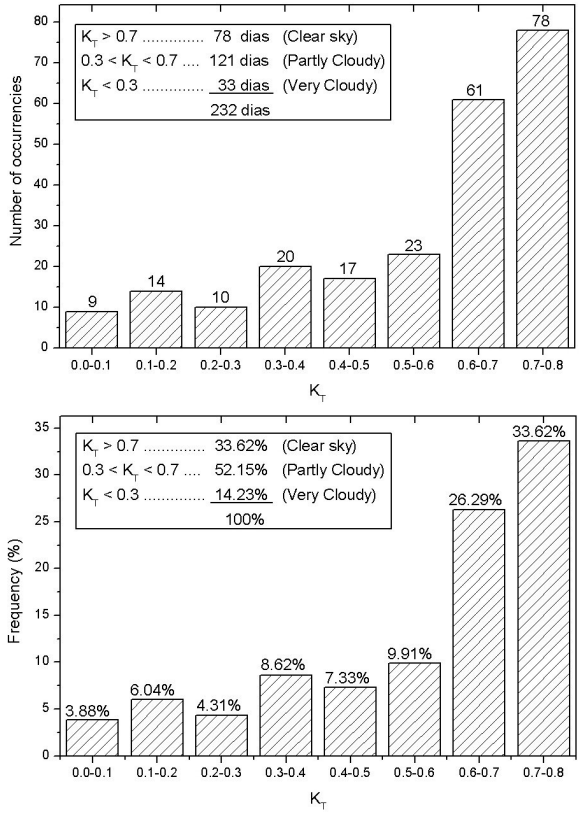

Figure 8 – Histograms of number (a) and percentage (b) of days in each clearness parameter interval.

Conclusions

Some preliminary results using global and diffuse radiation data from the São Martinho da Serra SONDA station were presented in this work. A good agreement between the observational data and the correlations created by Ruth and Chant (1976) and Collares-Pereira and Rabl (1979) was observed. Also, the daily diffuse radiation (expressed by K_d) behavior, as function of the clearness parameter (K_T), was the similar to that presented by Iqbal (1983).

Some deviations observed between observational and theoretical data were discussed. The diffuse radiation measurements in clear sky days presented values smaller than that indicated by other researchers. The latitude and atmospheric composition differences may be the possible causes of these differences.

Also, some days with a spurious behavior observed on Figures 5 and 6 are possibly related to the totally opposite cloudiness conditions observed along these days. To minimize this problem, new studies using hourly, instead of daily radiation data, are planned, as the correlations made by Pereira et al. (1996) for a Brazilian station.

The authors plan to create correlations for this station similar to those done by Ruth and Chant, and Collares-Pereira and Rabl. The availability of a larger period of data will make it possible. Also using data from all possible SONDA stations, it is expected to create a correlation that relates the diffuse and global radiation for the whole Brazilian area.

References

Brasseur, G., Solomon, S., 1986, Aeronomy of the Middle Atmosphere: D. Reidel Publishing Company, Dordrecht, Holland, 452p.

Collares-Pereira, M., Rabl, A., 1979, The average distribution of solar radiation correlations between diffuse and hemispherical and between daily and hourly insolation values: Solar Energy, Vol. 22 (2), p155-164.

Coulson, K. L., 1975, Solar and Terrestrial Radiation: Methods and Measurements: Academic Press, New York, 322 p.

Hoyt , D. V., Schatten, K. H., 1997, The role of the sun in climate change: Oxford University Press, New York.

Iqbal, M., 1983, An Introduction to Solar Radiation: Academic Press Canada, Toronto, 390p.

Iqbal M., 1979, Correlation of average diffuse and beam radiation with hours of bright sunshine: Solar Energy, Vol. 23 (2), p169-173.

Kidder, S. Q., Vonder Haar, T. H., 1995, Satellite Meteorology: an introduction: Academic Press, San Diego, 466p.

Kondratyev, K. Ya., 1969, Radiation in the Atmosphere: Academic Press, New York, 912p.

Lenoble, J., 1993, Atmospheric Radiative Transfer*:* A DEEPAK Publishing, Hampton, Virginia, USA, 532p.

Liou, Kuo-Nan, 1980, An Introduction to Atmospheric Radiation: Academic Press, Inc., New York, 392p.

Liu, B. Y. H., Jordan, R. C., 1960, The interrelationship and characteristic distribution of direct, diffuse and total solar radiation: Solar Energy, Vol. 4 (3), p1-19.

Lutgens, F. K.; Tarbuck E.J., 1989, The Atmosphere: an introduction to Metorology: Sixth Edition, Prentice Hall, Inc., New Jersey, 462p.

Peixoto J. P.; Oort, A. H., 1992, Physics of Climate: American Institute of Physics, AIP Press, 520p.

Pereira, E. B., Abreu, S. L., Colle, S., 1996, Determinação de uma correlação para o cálculo da radiação solar difusa incidente a partir da radiação solar global: Anais do VI Congresso Brasileiro de Engenharia e Ciências Térmicas, Florianópolis - SC, 11-14 de novembro.

Ruth, D. W., Chant, R. E., 1976, The relationship of diffuse radiation to total radiation in Canada: Solar Energy, Vol. 18 (2), p153-154.

Spencer, J. W., 1971, Fourier series representation of the position of the Sun: Search, Vol. 2 (5), p172.

Wallace, J. M., Hobbs, P. V., 1977, Atmospheric Science: an introductory survey: Academic Press, San Diego, 467p.

Acknowledgments

The authors would like to thank to CNPq and FINEP (Projeto SONDA – 22.01.0569.00) for the financial support. We are also grateful to the people involved in installation and maintenance of the SONDA stations, especially to who works at Observatório Espacial do Sul and the SONDA station installed there. R.A.G. thanks to Fernando Luis Guarnieri by the suggestions and improvement in this text.

Corresponding author. Address: Instituto Nacional de Pesquisas Espaciais – INPE, Prédio do DGE, Sala 12, Av. dos Astronautas, 1758 – Jardim da Granja – Caixa Postal 515 – CEP 12245-970 – São José dos Campos – SP – Brazil. Tel.: (12) 3945-6738.

E-mail address: ricardog@cptec.inpe.br (R. A. Guarnieri)
eniobp@cptec.inpe.br (E. B. Pereira)